American Mineralogist, Volume 75, pages 1043–1058, 1990

Rock pressure vs. fluid pressure as a controlling influence on mineral stability: An example from New Mexico

M. J. HOLDAWAY, J. W. GOODGE
Department of Geological Sciences, Southern Methodist University, Dallas, Texas 75275-0395, U.S.A.

ABSTRACT

A graphite-absent sequence of quartzite and schist on the north flank of the Picuris Range in north-central New Mexico provides a natural laboratory to test the thesis of Bruton and Helgeson that fluid pressure (P_f) is the effective pressure on solid phases during metamorphism. We have studied the Hondo Canyon and Section 8 areas of this range in detail. The presence of kyanite reacting to sillimanite in Ortega Formation quartzites and of andalusite reacting to sillimanite in neighboring Rinconada Formation schists may be explained by an effective pressure difference of 200 ± 100 bars between the two units. Composition, redox, T, and P_r (rock pressure) can all be ruled out as controlling factors, leaving a difference in P_f as the most likely cause of the differences in the mineral assemblages.

The presence of chloritoid + kyanite in the Ortega quartzite and staurolite in the adjacent jacent Rinconada schists can best be explained by bulk compositional effects. The schists have a higher bulk ratio of Mg/(Mg + Fe) than the quartzites, which allows staurolite and biotite to be stable at lower temperatures relative to chloritoid and muscovite than in the quartzites. In the absence of chloritoid, staurolite has higher R^{2+} and lower H content than would be expected in the quartzites. The concurrent reduction of tetrahedral vacancies reduces the activity of staurolite relative to the reaction chloritoid + kyanite = staurolite + quartz + fluid and stabilizes staurolite in the Rinconada schists. This reaction has a steep P-T slope that permits but does not require differences in P_f between the two units at constant T.

A difference in P_f of 200 ± 100 bars between the two rock types can best be explained by a contrast of permeability between the quartzites and mica schists, because the preferred orientation of minerals and planar grain boundaries in the micaceous rocks favor greater and more rapid fluid flow. P_f builds up to values closer to lithostatic pressure in the quartzites than in the mica-rich rocks. In fluid-present systems during low- and medium-grade metamorphism generally, the effective pressure on solid minerals appears to be fluid pressure rather than rock pressure.

INTRODUCTION

In the study of natural metamorphic rock systems, as thermodynamic data and thermobarometric calibrations become more accurate, it is important to select the most meaningful variables for determination of metamorphic conditions. Petrologists have experienced considerable difficulty relating the various metamorphic pressure variables (P_r, P_f, P_1, P_2, P_3) to each other and to mineral stability (Turner, 1980). The problem stems partly from the difficulty in relating fluid pressure (P_f) to rock pressure (P_r) theoretically, and partly from the limited information we can obtain directly from mineral assemblages. P_r, rock pressure, is defined by the bulk density and thickness of overlying rock, whereas P_f, fluid pressure, is the sum of the various fluid component pressures, $P_{H_2O} + P_{CO_2} + P_{CH_4} + \ldots$. The general approach has been either to assume that $P_r = P_f$, an assumption that is so routinely made that it is commonly not even mentioned, or to try to calculate P_r from solid-solid mineral reactions and P_f from solid-fluid reactions and then compare the two. This approach has the disadvantage that most of the error of the calibration and calculations is included in the value of P_r-P_f, and one cannot be sure that P_r-P_f is not zero. If in fact $P_r \neq P_f$, then the question arises as to which pressure variable is the effective thermodynamic pressure constraint on solid phases.

Bruton and Helgeson (1983) used the approach of Gibbs (1878) to characterize equilibria among nonhydrostatically stressed solids coexisting with hydrostatically stressed fluids in a variety of hydrothermal systems. They concluded that under crustal conditions phase relations are essentially independent of P_r and the effective thermodynamic pressure on all solid phases is P_f. If this is the case, P_r may be ignored from the petrologic standpoint, and the only pressure that can be related to mineral stabilities is P_f. This also could simplify the debate regarding

0003–004X/90/0910–1043$02.00

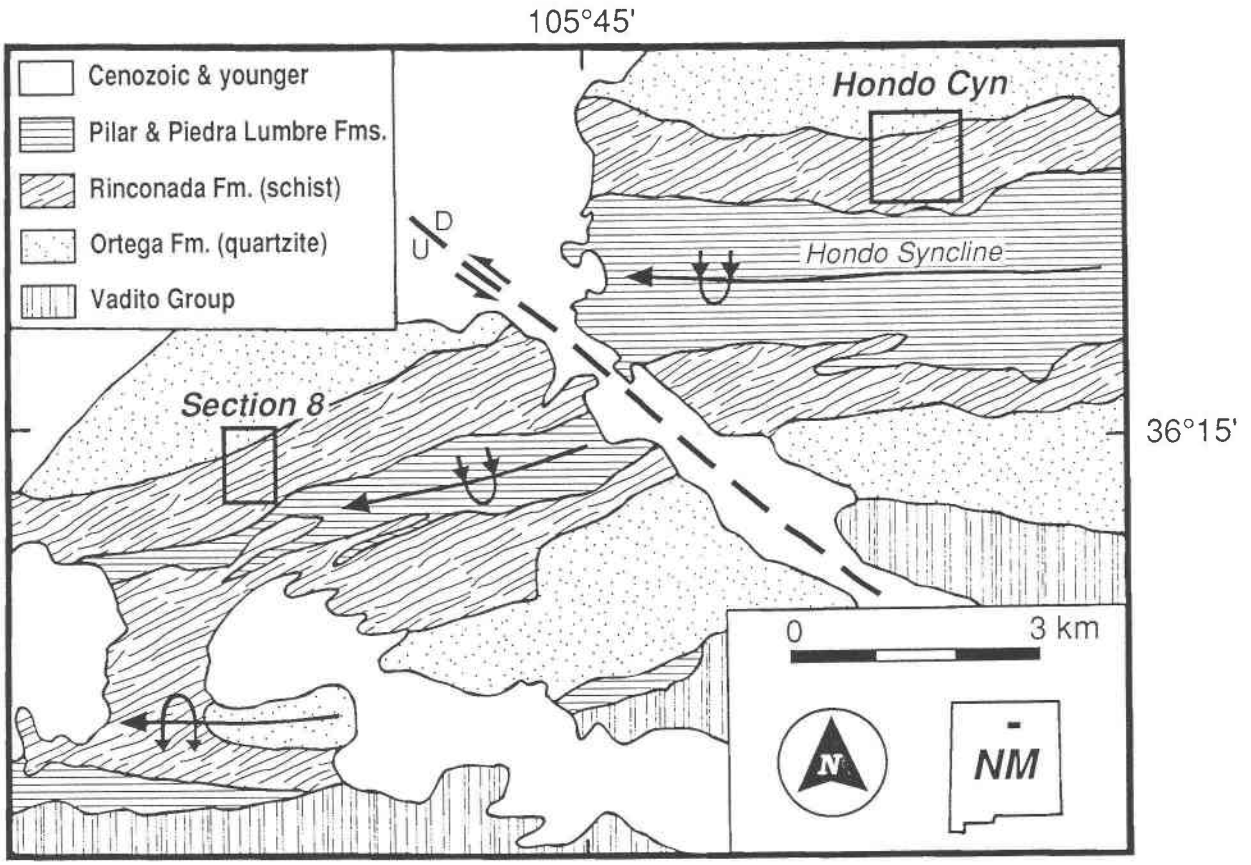

Fig. 1. Generalized geology of the northern Picuris Range, New Mexico (after Montgomery, 1953; Nielson, 1972; Bauer, 1984). Piedra Lumbre, Pilar, Rinconada and Ortega units are part of Proterozoic Ortega Group (Bauer and Williams, 1989), and are stratigraphically underlain by ~1.7 Ga rocks of the Vadito Group. Heavy broken line is trace of Pilar-Vadito fault. Locations of areas in Figures 2 and 3 outlined by boxes.

the relation between effective thermodynamic pressure and the three principal stresses (P_1, P_2, P_3) in a nonhydrostatically stressed solid (Kamb, 1961; Verhoogen, 1951; MacDonald, 1957), because P_f has no direct relation to any principal stress. The meaningful pressure variables become P_f, P_1, P_2, and P_3. Etheridge et al. (1984), Norris and Henley (1976), and Fyfe et al. (1978) have summarized evidence to show that during regional metamorphism $P_f \approx P_3$, the minimum principal stress. However, there is no reason to believe that P_f must be uniform on a local scale as P_r must be. The value of P_f during metamorphism depends on local variations in permeability and rates of fluid production and consumption in the rocks (Walther and Orville, 1982).

The paper of Bruton and Helgeson (1983) has received very little attention beyond casual citation since its publication. Among the more substantive commentary, Wheeler (1985) and Bayly (1987) have pointed out that Bruton and Helgeson assumed that the fluid phase against a nonhydrostatically stressed solid is under hydrostatic pressure, and this may not be strictly true. Rutter and Brodie (1988a, 1988b) cite experiments that show that the serpentine decomposition temperature decreases at constant P_{H_2O} as P_r is increased, suggesting that P_r may have an effect on mineral stability. However, their experiments show that with increasing P_r the dehydration temperature decreases to a constant value rather than at a constant rate. In addition, the experiments were carried out under conditions of differential stress and may not be directly applicable to simple hydrostatic systems. We are aware of no attempt to verify the treatment by Bruton and Helgeson (1983) on the basis of natural observations. In the example considered in this report, we provide arguments that the effective thermodynamic pressure on solid phases in fluid-present systems should be P_f, and then we attempt to show that this assumption indeed has merit by investigating Al_2SiO_5-bearing assemblages in Proterozoic metasedimentary rocks in north-central New Mexico that serve to monitor slight variations in pressure of equilibration.

Petrologic setting of the Picuris Range

The Picuris Range in north-central New Mexico (Fig. 1), 20 km southwest of Taos, is a westward extension of

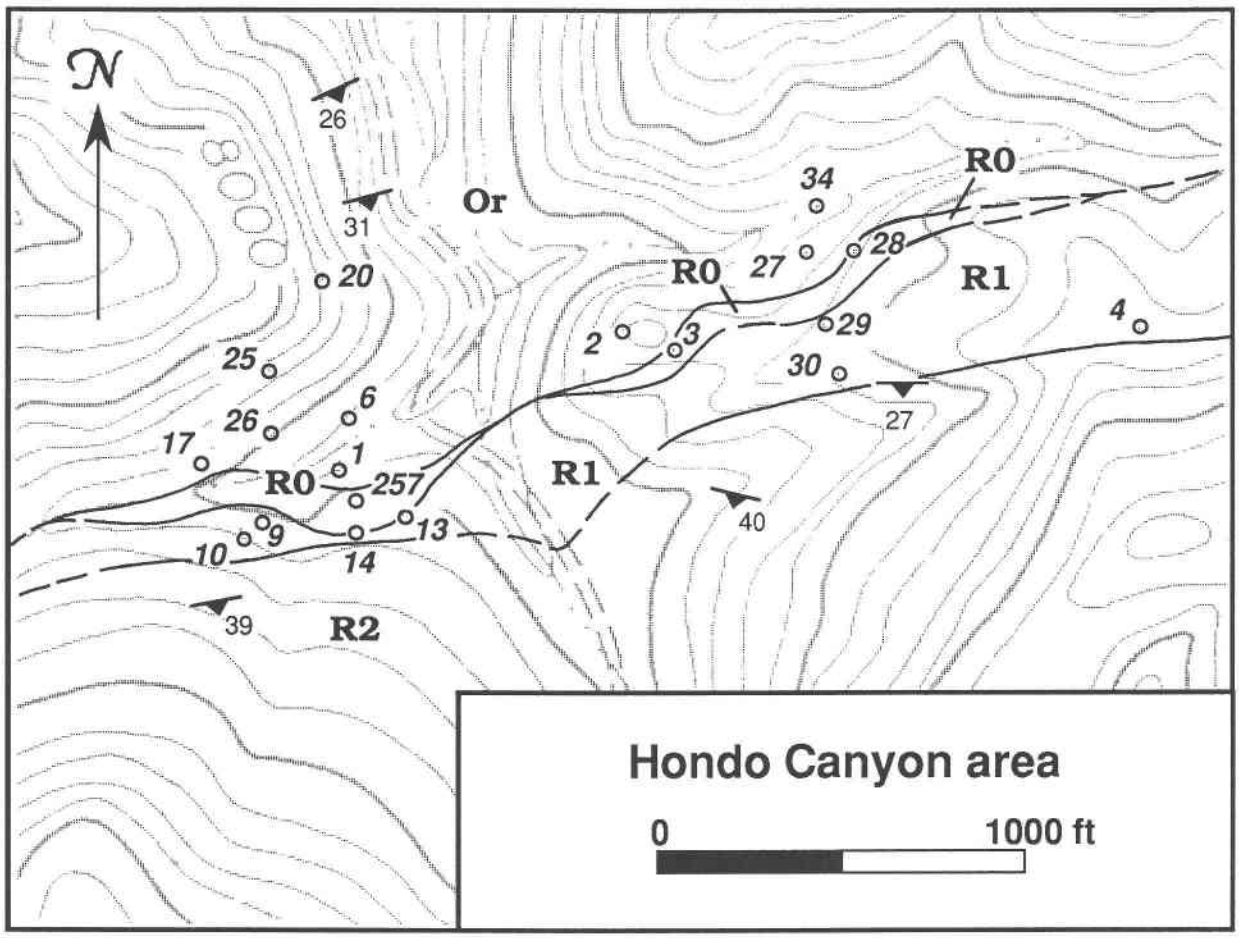

Fig. 2. Geologic map of the Hondo Canyon area (geologic mapping by C.L. Rattel-Carson, M.J. Holdaway, and J.W. Goodge). Or = Ortega Formation; R0–R2 = subunits of Rinconada Formation. Localities and numbers refer to specimens with mineral analyses given in Tables 2–4. Attitudes refer to schistosity, which is nearly parallel to bedding. Contour interval: 40 ft.

the Sangre de Cristo Mountains that provides a natural laboratory to test the concept of Bruton and Helgeson (1983). The value of the area lies in the likelihood that a single metamorphic event has produced all three Al_2SiO_5 polymorphs and both chloritoid and staurolite (Holdaway, 1978). Major east-trending folds and penetrative deformation predate the culmination of metamorphism at about 1400 Ma (J. A. Grambling, personal communication). Textures of the rocks indicate a static final stage of thermal recrystallization with no evidence of deformation during the peak of metamorphism (Nielsen, 1972; Holdaway, 1978).

Careful field work and sample collection were undertaken along the north flank of the range in two areas, Hondo Canyon and Section 8, located 8.8 km S 60°W of Hondo Canyon (Figs. 2, 3). In each of these areas, massive quartzites of the Ortega Formation (Bauer and Williams, 1989) lie stratigraphically beneath pelitic schists and interlayered micaceous quartzites of the Rinconada Formation. The units dip uniformly south at about 30–60° within the northern upright limb of an overturned syncline (Fig. 1). Chloritoid and kyanite are prevalent in the Ortega quartzites, whereas staurolite and andalusite are widespread in the lower Rinconada schist subunits. Sillimanite may be found in both formations, and andalusite also occurs locally in the Ortega quartzites. Elsewhere in the Picuris Range chloritoid, kyanite, and andalusite are present in the Ortega, and staurolite, and locally andalusite, occur in the lower Rinconada (Holdaway, 1978).

Mineral assemblages of the Ortega and lower Rinconada subunits in the two areas (Figs. 2, 3) are summarized in Table 1. The Ortega is principally quartzite with locally developed thin, discontinuous horizons of kyanite (oriented parallel to schistosity), muscovite, and most or all of the other minerals shown. The R0 subunit of the Rinconada Formation has not been previously described and is a thin, discontinuous granoblastic rock, containing 30–50% staurolite, and lacking garnet, chloritoid, and Al_2SiO_5. An abrupt transition from quartz-dominated

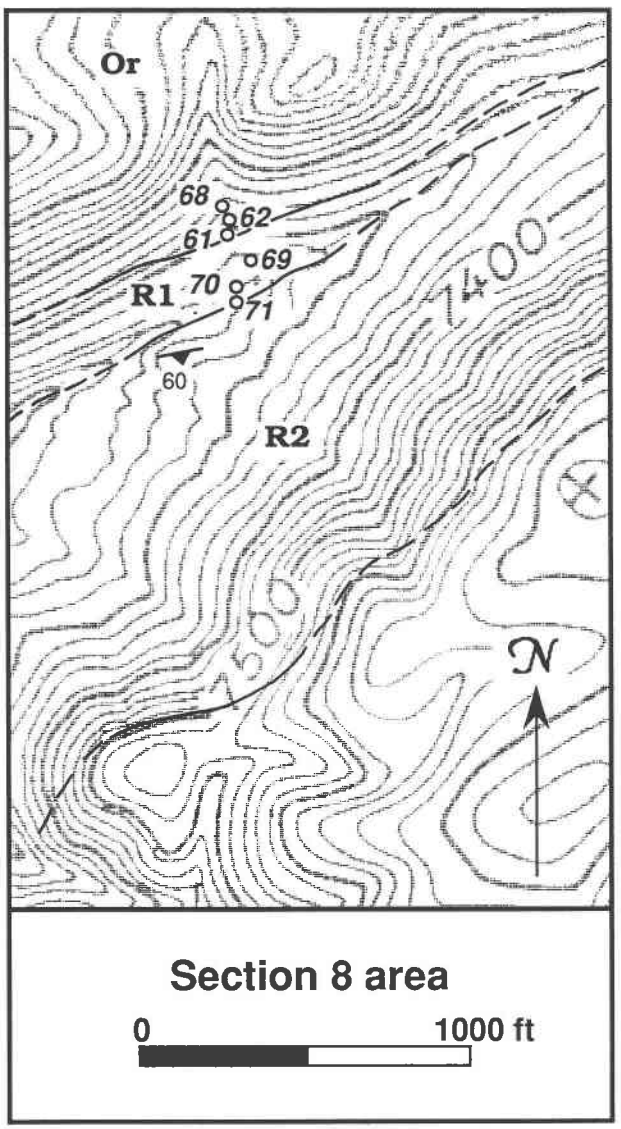

Fig. 3. Geologic map of the Section 8 area (geologic mapping by C.L. Rattel-Carson, M.J. Holdaway, and J.W. Goodge). Or = Ortega Formation; R1, R2 = subunits of Rinconada Formation. Localities and numbers refer to specimens with mineral analyses given in Tables 2–4. Attitudes refer to schistosity, which is nearly parallel to bedding. Contour interval: 20 ft.

(Ortega Formation) to more micaceous rocks (Rinconada Formation) occurs at the base of R0. Fist-sized poikiloblasts of randomly oriented andalusite and smaller porphyroblasts of randomly oriented biotite and staurolite occur in R1. On the basis of mineral abundances and compositions, the sedimentary protoliths for the units probably contained resistate minerals, kaolinite, and minor illite in Ortega; kaolinite and illite in R0; illite in R1; and illite and organic material in R2. The present study considers only Ortega, R0, and R1, all of which contain a hematite-ilmenite oxide phase (ilmenite containing substantial hematite component) and no graphite. Holdaway (1978) provides textural evidence to suggest that all reactions involving Al_2SiO_5 polymorphs were largely the result of increasing T. Ortega kyanite and chloritoid probably grew before the peak of metamorphism, during an early phase of dynamic recrystallization, whereas unoriented andalusite, biotite, staurolite, and sillimanite probably grew under more static conditions at a time close to the peak of metamorphism.

Microprobe analyses of hematite-ilmenite, magnetite, Al_2SiO_5 polymorphs, staurolite, and chloritoid were undertaken using procedures described by Dickerson and Holdaway (1989, Appendix). Hematite-ilmenite, staurolite, and chloritoid were normalized to standards analyzed every 1–1.5 h to minimize spectrometer and electronic drift. Estimated precision is 1–2 mol% of major components. Staurolite stoichiometry was based on Si + Al = 25.53 (Holdaway et al., 1986a).

The only cations detected in hematite-ilmenite are Fe, Ti, Mn, and Mg, whereas Al, Si, and Fe are the only components >0.001 atoms pfu in the Al_2SiO_5 polymorphs (Table 2). The presence of magnetite or rutile is shown in Table 2. Magnetite contains trace Mg and Al and between 0 and 1.5 mol% ulvöspinel solid solution. Chloritoid in Ortega quartzite varies in the ratio Mg/(Mg + Fe_{tot}) from 0.01 to 0.09 and in the ratio Mn/(Mn + Mg + Fe_{tot}) from 0.004–0.050. Mn is higher in chloritoids with more Mg (Table 3), possibly reflecting variation in trioctahedral illite component, with more Mg and Mn. Staurolite from R0 has Mg/(Mg + Fe_{tot}) = 0.15–0.19, and that from R1 has Mg/(Mg + Fe_{tot}) = 0.21–0.26 (Table 4). Staurolite from the reduced R2 unit, with coexisting graphite and ilmenite (Table 1), has Mg/(Mg + Fe_{tot}) = 0.12–0.18 (unpublished data). A single Ortega specimen contains Fe-rich staurolite with Mg/(Mg + Fe) = 0.005.

Intensive variables and related assumptions

Garnet-biotite geothermometry on R2 (which contains graphite and pure ilmenite) using the calibration of Ganguly and Saxena (1984) with P = 3.8 kbar and ΔW_{Mn} = 2500 cal/mol (the value used by Holdaway et al., 1988) gives 532 ± 30 °C for six specimens from Hondo Canyon and 529 ± 30 °C for five specimens from Section 8, based on unpublished data of Goodge and Holdaway. The T standard deviation of ±30° results mainly from analytical precision and minor disequilibrium, as opposed to real variation in temperature (Holdaway et al., 1988). There must have been a small, finite range of T within each area. There is no obvious correlation of T variation with structural or stratigraphic position in either area. Most of the mineralogic differences between units (Tables 1–4) can be related to stratigraphic compositional differences in protolith and not to T. For the purpose of estimation of P and T in the section that follows, we assume a T range of 4° in each area. Larger or smaller values could be assumed with no appreciable effect on our results. Greater frequency of sillimanite in Hondo Canyon than in Section 8 implies that T may have been a few degrees

TABLE 1. Mineral assemblages of subunits in Hondo Canyon and Section 8

Subunit	Assemblage
R2	Ms + Qz + Bt + St + Alm + Ilm + Gr (+Pl)
R1	Ms + Qz + Bt + And + Sps (+St) + Hl (+Sil) (+Mag) (+Pl)
R0*	St + Ms + Qz + Bt + Hl (+Mag) (+Sil)
Or	Qz + Ky + Ms (+Sil) + Hl (+Cld) (+Mag) (+Rt) (+And) (+St)

Note: Or = Ortega, R = Rinconada; mineral abbreviations after Kretz (1983). Minerals are listed in average order of decreasing abundance (see also Table 2). Parentheses indicate mineral absent from some (or most) specimens. Sps indicates garnet with substantial spessartite component. Hl indicates hematite-ilmenite. Tourmaline is also present in many specimens.

* R0 unit is not present in Section 8 area (Fig. 3).

lower in Section 8 than in Hondo Canyon, as discussed below.

During metamorphism P_r may be assumed to have been very nearly constant within each of the two areas because of the very limited scale involved (a stratigraphic and structural thickness of ~100 m; Table 2) and the lack of syn- or postmetamorphic deformation. Small differences in P_r within each area relate to elevation differences and a present-day regional dip of isobaric surfaces estimated at 3° to the west by Grambling (1988). Taking these two factors into account, P_r may have varied over a total range of 40 bars in Hondo Canyon and 10 bars in Section 8. These ranges may be assumed to be minimum ranges for P_f within a single stratigraphic unit with approximately uniform permeability.

If we assume negligible external sources or sinks of CO_2 and CH_4, the graphite-ilmenite-bearing rocks of R2 maintained f_{O_2} at values near the FMQ buffer by reaction of H_2O (from dehydration reactions) with graphite to produce CH_4 and CO_2 in comparable amounts (Ohmoto and Kerrick, 1977; Holdaway et al., 1988). On the other hand, Ortega quartzite and Rinconada units R0 and R1 contain no graphite or carbonates. Thus the fluid in these units may be assumed to have been nearly pure H_2O.

Hematite-ilmenites in Ortega, R0, and R1 may be grouped in three compositional ranges: (1) hematites in

TABLE 2. Mineral assemblages and stoichiometry of oxides and Al_2SiO_5 polymorphs*

Specimen	Elev. (m)	Strat. dist. (m)	Unit	Cld/St	Mag/Rt	Hem	Ilm	Mn-Ilm	Mg-Ilm	Fe-And	Fe-Ky	Fe-Sil
						Hondo Canyon						
4	2466	47.5	R1	St	—	0.062	0.908	0.021	0.009	0.030	—	Pr
30	2429	44.2	R1	St	—	0.749	0.243	0.008	0.000	0.030	—	0.014
10	2304	40.2	R1	—	Mag	0.731	0.263	0.006	0.000	0.030	—	0.027*
29	2428	28.3	R1	St	—	(0.000)	(0.926)	(0.074)	(0.000)	0.030	—	0.041*
9	2380	26.5	R1	St	—	0.027	0.757	0.216	0.000	0.026	—	0.013
13	2382	25.3	R1	St	Mag	0.752	0.245	0.003	0.000	0.030	—	Pr
14	2387	22.9	R0	St	Mag	(0.051)	(0.947)	(0.002)	(0.000)	—	—	—
257A	2380	7.0	R0	St	Mag	(0.000)	(0.998)	(0.002)	(0.000)	—	—	—
3	2420	4.6	R0	St	Mag	0.116	0.864	0.015	0.005	—	—	—
28	2423	3.0	R0	St	Mag	(0.051)	(0.941)	(0.005)	(0.003)	—	—	Pr
1	2365	−0.6	Or	Cld	—	0.888	0.110	0.001	0.001	—	—	0.021
17	2387	−0.9	Or	—	—	0.628	0.372	0.000	0.000	—	0.009	0.011
26	2379	−1.5	Or	Cld	—	0.720	0.280	0.000	0.000	—	0.012	0.017
6	2364	−1.8	Or	—	Rt	(0.066)	(0.928)	(0.006)	(0.000)	—	0.008	—
25	2408	−3.0	Or	CldSt	—	(0.000)	(0.999)	(0.001)	(0.000)	—	0.007	0.013
20	2411	−5.5	Or	Cld	Rt	0.649	0.351	0.000	0.000	—	0.010	0.008
27	2408	−21.6	Or	Cld	—	0.816	0.184	0.000	0.000	0.032	0.017	0.016
2	2426	−28.3	Or	Cld	—	0.767	0.233	0.000	0.000	—	0.009	0.017
34	2397	−44.8	Or	Cld	Rt	0.627	0.373	0.000	0.000	—	0.009	0.012
						Section 8						
71	2211	45.7	R1	St	—	0.695	0.297	0.005	0.003	0.031	—	—
70A	2213	36.6	R1	—	—	Pr	—	—	—	0.030	—	—
69	2217	19.8	R1	St	—	Pr	—	—	—	—	—	—
61A**	2224	−0.3	Or	—	Mag	0.638	0.349	0.003	0.010	0.026	0.013	—
61C	2224	−0.9	Or	—	Mag	0.631	0.348	0.010	0.011	0.032	0.013	—
61G	2225	−2.1	Or	—	Mag	0.693	0.298	0.000	0.009	—	0.010	—
61H	2225	−3.7	Or	Cld	Mag	0.737	0.260	0.003	0.000	—	0.011	0.012
62	2228	−12.2	Or	Cld	Mag	0.670	0.330	0.000	0.000	—	0.012	Pr
68	2234	−24.4	Or	—	Rt	0.677	0.310	0.000	0.013	—	0.011	—

Note: Hem and Ilm represent mole fractions of hematite and ilmenite component, respectively. Mn-Ilm, Fe-And, etc., represent number of atoms of Mn or Fe pfu. In Al_2SiO_5 polymorphs the remaining atoms are Al, such that Fe + Al = 2. Numbers in parentheses represent hematite-ilmenites that have suffered Fe loss by exsolution/oxidation as indicated by low oxide totals and visible exsolution lamellae. Primary hematite component is estimated to be 5–10% more than analyzed values. Pr indicates mineral is present but could not be analyzed.

* Fibrolitic, assumed to be disequilibrium.

** Specimen contains trace iron davreauxite(?); analysis given in Table 3.

TABLE 3. Chemical analyses and stoichiometry of chloritoid and iron davreauxite (61A) in Ortega Formation quartzite samples

Specimen	1	25	20	27	2	34	61H	62	61A
SiO_2	23.56	23.79	23.64	23.56	23.03	23.56	23.36	23.51	26.90
Al_2O_3	40.21	39.78	39.82	40.30	39.88	40.06	40.09	39.49	53.83
TiO_2	0.00	0.02	0.00	0.00	0.00	0.05	0.02	0.02	0.45
FeO	26.49	28.62	27.13	26.93	25.39	27.35	26.31	27.20	8.88
MgO	1.23	0.15	0.82	0.46	1.39	0.52	0.65	0.48	0.48
MnO	0.56	0.11	0.33	0.27	1.52	0.25	1.05	0.42	0.38
Total	92.05	92.46	91.73	91.53	91.21	91.79	91.48	91.12	90.92
				Cations on the basis of 8 cations					**21 cations**
Si	1.975	2.006	1.996	1.995	1.947	1.992	1.980	2.003	5.708
Al	3.977	3.954	3.966	4.023	3.976	3.994	4.004	3.971	13.475
Ti	0.000	0.000	0.000	0.000	0.000	0.002	0.000	0.000	0.024
Fe	1.857	2.017	1.915	1.907	1.795	1.934	1.864	1.938	1.572
Mg	0.152	0.017	0.102	0.057	0.174	0.063	0.081	0.059	0.147
Mn	0.038	0.007	0.021	0.018	0.108	0.015	0.072	0.029	0.063
Mg/(Mg + Fe)	0.078	0.008	0.051	0.029	0.092	0.032	0.042	0.030	0.086

Ortega and R1 with a hematite component between 0.63 and 0.89, (2) three ilmenites in R0 and R1 with a hematite content of 0.03–0.12, and (3) six ilmenites in all three units with observable fine exsolution, average Ti contents (2-cation basis) between 0.93 and 1.06, and oxide totals (assuming all Fe as FeO) of 94.3–97.5 wt%. This latter phase appears to have suffered retrograde exsolution, oxidation, and Fe loss such that its prograde composition cannot be determined with certainty. Combining our data on unaltered oxides with those of Grambling (1981, 1986) for rocks that formed at about the same P and T, we suggest that the hematite immiscibility noted by Grambling extends between approximately $Hem_{0.20}$ and $Hem_{0.63}$ at 530 °C.

Hematite-ilmenite cannot be used as a precise indicator of f_{O_2} unless another Ti or Fe phase is present. Rutile is absent from most specimens, but magnetite is present in several (Table 2). Despite the fact that the magnetite is nearly pure, the Spencer and Lindsley geothermometer and O geobarometer (1981, Fig. 4) may be used to estimate f_{O_2} by assuming a T of 530 °C. Unfortunately, the grid is not very accurate at low T in the vicinity of the hematite-ilmenite miscibility gap. Magnetite-bearing specimens have indicated f_{O_2} values between approximately 10^{-18} and 10^{-19}. As long as the composition of hematite-ilmenite coexisting with magnetite does not approach pure ilmenite or pure hematite, the wide range of composition does not require a wide range of f_{O_2}, because the miscibility gap must produce a tight grouping of isopleths one to two log units below the HM buffer, analogous to the magnetite-ulvöspinel isopleths near $f_{O_2} = 10^{-25}$ (Spencer and Lindsley, 1981, Fig. 4). Values of f_{O_2} between $10^{-22.1}$ and $10^{-23.7}$, calculated by Grambling (1986) for ilmenites with very low hematite component in rocks that formed at nearly the same P and T, were based on the Gibbs method (Spear et al., 1982). Grambling used rutile as the coexisting phase and assumed ideal mixing for hematite-ilmenite. This approach gives precise results

TABLE 4. Chemical analyses and stoichiometry of staurolite*

Unit	R1	R1	R1	R1	R1	R0	R0	R0	R0	Or	R1	R1
Specimen	4	30	29	9	13	14	257A	3	28	25**	71	69
SiO_2	27.28	27.18	27.38	27.19	27.02	27.43	27.39	27.00	27.10	28.61	27.33	27.55
Al_2O_3	53.84	53.11	53.54	53.42	53.82	54.53	54.77	53.10	53.33	56.35	53.42	53.85
TiO_2	0.49	0.53	0.50	0.58	0.51	0.50	0.48	0.46	0.63	0.22	0.46	0.46
FeO	11.99	13.63	13.18	13.61	12.37	13.58	13.67	15.32	15.05	10.90	11.69	13.46
MgO	2.03	2.04	2.42	2.35	2.26	1.36	1.54	2.04	1.80	0.03	2.28	2.23
MnO	0.53	0.67	0.67	0.62	0.77	0.16	0.12	0.23	0.21	0.05	0.77	0.55
ZnO	1.82	1.11	0.68	0.50	1.50	0.11	0.09	0.06	0.12	0.13	2.25	0.19
Total	97.98	98.26	98.36	98.28	98.26	97.67	98.07	98.20	98.25	99.81	98.19	98.29
				Cations on the basis of (Si + Al) = 25.53						**48 O**		
Si	7.676	7.730	7.721	7.696	7.628	7.638	7.605	7.695	7.692	7.786	7.725	7.729
Al	17.854	17.800	17.809	17.834	17.902	17.892	17.925	17.835	17.838	18.069	17.805	17.802
Ti	0.099	0.113	0.104	0.115	0.105	0.105	0.101	0.099	0.135	0.046	0.091	0.090
Fe	2.813	3.240	3.112	3.217	2.916	3.161	3.175	3.651	3.571	2.479	2.762	3.154
Mg	0.847	0.859	1.014	0.989	0.945	0.564	0.636	0.865	0.763	0.012	0.953	0.930
Mn	0.124	0.158	0.157	0.141	0.182	0.038	0.028	0.056	0.050	0.012	0.183	0.132
Zn	0.371	0.226	0.141	0.099	0.307	0.023	0.018	0.013	0.025	0.026	0.464	0.033
H + Li	3.028	2.263	2.424	2.364	2.662	3.780	3.685	2.151	2.361	5.409	2.597	2.825
Mg/(Mg + Fe)	0.232	0.210	0.246	0.235	0.245	0.151	0.167	0.192	0.176	0.005	0.257	0.228

* H + Li is estimated by subtracting the total positive charge from 96 (Holdaway et al., 1988) and has an estimated error (2σ) of 0.8. Estimated Li is 0.2 atoms pfu in all staurolites except specimen 25.

** Ion probe analysis by Richard Hervig, $Li_2O = 1.42$, $H_2O = 2.1$; Li = 1.566, H = 3.843.

only for a narrow composition range near pure ilmenite. The accuracy of the method depends on the calibration, for which Grambling used a titaniferous hematite; the assumption of ideal solid solution may have affected the quality of the calibration. Our specimens with $Hem_{0.027}$ and $Hem_{0.062}$ coexist with neither magnetite nor rutile and thus cannot be used to estimate f_{O_2}. These must be more ilmenite-rich than the composition stable with magnetite at the same f_{O_2} (Spencer and Lindsley, 1981, Fig. 2).

Given the small allowable differences in f_{O_2} with hematite-ilmenite composition we can now discuss relative differences in f_{O_2} between Ortega, R0, and R1. We note that in general magnetite-bearing specimens should contain the most Fe-rich hematite-ilmenite for a given f_{O_2}, rutile-bearing assemblages should contain the most Fe-poor hematite-ilmenite, and hematite-ilmenite with neither oxide is presumably intermediate between these extremes. Based on a comparison between the chemistry of the unaltered and altered ilmenites, we estimate that the six altered ilmenites are probably 5–10 mol% richer in ilmenite component than their prograde equivalents. If one takes all these things into account (Table 2), Ortega is most oxidized on average, followed by R1, then R0, and finally R2 (with pure ilmenite, Goodge and Holdaway, unpublished data). Several important observations thus bear on the relative f_{O_2} of these units: (1) there was no systematic gradient in f_{O_2} from Ortega to R2; (2) significant variations in f_{O_2} occurred in R1 and perhaps Ortega over short distances; (3) R2 was the only unit with distinctly low values of f_{O_2}; and (4) individual specimens of Ortega, R0, and R1 overlapped each other.

The most significant intensive variable in Ortega quartzite, R0, and R1 may have been P_f, and this fluid was largely H_2O as discussed above. Differences in P_f may be expected between the quartz-dominated Ortega quartzite and the mica-dominated Rinconada subunits. Significant differences in permeability are possible between various crystalline rock types (Brace, 1980), as are differences in volatile production (Walther and Orville, 1982). Randomly oriented tight quartz grain boundaries in the quartzite would allow less rapid and pervasive fluid flow than along planar mica boundaries in the Rinconada rocks, which show a degree of preferred orientation inherited from deformation during low-grade metamorphism. In the treatment that follows, we allow P_f to vary among units. As mentioned above, we consider that estimates of the range of P_r in each area serve as minimum estimates of the range of P_f, which otherwise may vary as a function of fluid production, fluid consumption, total fluid flux, and permeability.

In summary, we make the following assumptions for Ortega quartzites and Rinconada Formation subunits R0 and R1: (1) in each area T varied randomly over approximately 4 °C; (2) the maximum range of P_r was 40 bars in Hondo Canyon and 10 bars in Section 8; (3) f_{O_2} did not vary significantly; (4) the fluid phase was nearly pure H_2O; and (5) P_f varied between rocks of the Ortega and Rinconada Formations, but within individual units, minimum ranges of P_f were 40 bars in Hondo Canyon and 10 bars in Section 8.

Determination of T and $P_f = P_{H_2O}$

In order to show that P_f does indeed vary between the Ortega and Rinconada units we will consider two types of equilibria: those among Al_2SiO_5 phases and those between chloritoid and staurolite.

Equilibria involving Al_2SiO_5

The solid-solid equilibria among Al_2SiO_5 polymorphs may be used very effectively, presuming equilibrium was attained, to constrain P_f-T conditioned in the Ortega and R1 units. These equilibria cannot be applied to the staurolite-rich R0 subunit, which contains no Al_2SiO_5 phase. Under the oxidizing conditions of Ortega quartzite and R1, with very low bulk Mn content, the equilibria involving Al_2SiO_5 are made slightly divariant by selective partitioning of Fe between phases. In order to study the effects of Fe partitioning, we make two simplifying assumptions: (1) Fe^{3+} partitions evenly between Al sites in each phase; (2) a Nernst distribution coefficient (K_n) may be used for Fe partitioning between phases without introduction of significant error.

Winter and Ghose (1979) showed that the Al sites in kyanite are all octahedral and about the same size, whereas in sillimanite the $^{[6]}$Al sites are significantly (9%) larger than the $^{[4]}$Al sites, and $^{[6]}$Al sites in andalusite are significantly (6%) larger than the $^{[5]}$Al sites. This suggests that Fe might partition evenly into Al sites in kyanite and into only one of two sites in sillimanite and andalusite. However, Grew (1980) has shown that the partitioning of Fe^{3+} between sillimanite and ilmenite is best explained by solid solution on both Al sites of sillimanite. On the other hand, Kerrick and Speer (1988) used a one-site model for sillimanite and andalusite, and Grambling and Williams (1985) assumed a single Al site is involved in solid solution for all three minerals. Our work cannot shed any light on this, but because of the small amounts of solid solution and the low concentration of Mn, we assume a simple two-site model based on Fe^{3+} substitution for all Al in each of the polymorphs. Experimentation with the data of Table 2 shows that for the Fe contents observed, more sophisticated models would have no effect on the results.

By the same argument, the dilute solid solutions lend themselves to formulation of the Nernst distribution coefficient (K_n), a simple procedure which gives the same results as distribution coefficients that take into account the dilution of Al. Thus, mole fractions of the end-member components for Al_2SiO_5 polymorphs are expressed as $X_{Al_2SiO_5}$ and $X_{Fe_2SiO_5}$ (note that the Fe values in Table 2 must be halved). Nernst distribution coefficients for each Al_2SiO_5 pair are given in Table 5, based on the present study and data of Grambling (1981) and Grambling and Williams (1985). Average K_n values from Table 5 may thus be used to calculate the composition of an Al_2SiO_5

TABLE 5. Partitioning of Fe between Al_2SiO_5 polymorphs at about 530 °C*

Specimen	Andalusite $X_{Fe_2SiO_5}$	Kyanite $X_{Fe_2SiO_5}$	Sillimanite $X_{Fe_2SiO_5}$	References**
9	0.013		0.065	1
30	0.015		0.007	1
27	0.016	0.0085	0.008	1
77-324	0.020	0.010	0.010	2
78-105A	0.019	0.008	0.009	3
61A	0.013	0.0065		1
61C	0.016	0.0065		1
77-47	0.015	0.005		2
78-96	0.019	0.0075		3
78-103	0.0165	0.0075		3
C6	0.002	0.0015		3
C18	0.001	0.0005		3
61H		0.0055	0.006	1
17		0.0045	0.0055	1
26		0.006	0.010	1
25		0.0035	0.0065	1
20		0.005	0.004	1
2		0.0045	0.0085	1
34		0.0045	0.006	1
76-472		0.005	0.005	2
76-529A		0.010	0.010	2
76-547		0.005	0.005	2
77-341A		0.005	0.010	2
80-99C		0.0015	0.001	3
80-217		0.0085	0.0095	3
81-176		0.001	0.001	3
C517A		0.001	0.001	3

$$\frac{X^{And}_{Fe_2SiO_5}}{X^{Sil}_{Fe_2SiO_5}} = 2.05,\ 2.00\dagger$$

$$\frac{X^{And}_{Fe_2SiO_5}}{X^{Ky}_{Fe_2SiO_5}} = 2.22,\ 2.30$$

$$\frac{X^{Sil}_{Fe_2SiO_5}}{X^{Ky}_{Fe_2SiO_5}} = 1.24,\ 1.15$$

* Three obvious disequilibrium pairs and all Mn-rich Al_2SiO_5 pairs are not tabulated.

** References: 1—this report, 2—Grambling (1981), 3—Grambling and Williams (1985).

† First figure is average value of K_n, second figure is average value adjusted within 1σ range to produce a mutually consistent set. Note that $X_{Fe_2SiO_5}$ values are one-half the values of Fe-And, etc. tabulated in Table 2 because Fe-And is based on two Al sites.

TABLE 6. Molar volumes and entropies of phases involved in Al_2SiO_5 reactions and Reaction 3

Mineral	Formula	$V^{298\ K}$ (J/bar)	$S^{800\ K}$ (J/K)	Notes
Kyanite	Al_2SiO_5	4.412	240.96	1
Sillimanite	Al_2SiO_5	4.983	252.75	1
Andalusite	Al_2SiO_5	5.147	249.80	1
Chloritoid	$Fe_2Al_4Si_2O_{10}(OH)_4$	13.934	840.66	2, 3
Staurolite	$H_4Fe_{3.6}Al_{17.92}Si_{7.66}O_{48}$	44.504	2667.81	4, 5
Quartz	SiO_2	2.269	98.27	1
Fluid	H_2O	2.179	134.60	6
Fluid	H_2O	2.231	135.33	7
Fluid	H_2O	2.260	135.73	8

Notes: 1—Berman (1988); 2—Ganguly and Newton (1968); 3—structural analogue, 2 pyrophyllite + 1 fayalite − 7 quartz; 4—unpublished unit-cell dimensions of specimen 71-62B (Black Mountain; Rumble, 1978) with about 4 H and Mg/(Mg + Fe) = 0.10; 5—Hemingway and Robie (1984) corrected for chemical differences and minimum disorder effects (Holdaway et al., 1988, Appendix); 6—527 °C, 4.4 kbar for V and S; 7—527 °C, 4.0 kbar for V and S; 8—527 °C, 3.8 kbar for V and S. All values for pure H_2O fluid from Burnham et al. (1969).

polymorph that would form by reaction of another Al_2SiO_5 phase of any given composition.

Following the same general procedure as used by Grambling and Williams (1985) and by Kerrick and Speer (1988), we can calculate a modified Al_2SiO_5 stability diagram in the vicinity of the triple point that takes into account the effect of Fe^{3+} on stability relations. Taking the reaction

$$\underset{\text{Andalusite}}{Al_2SiO_5} = \underset{\text{Sillimanite}}{Al_2SiO_5} \qquad (1)$$

as an example, the pressure shift from the pure phase diagram due to Fe^{3+} substitution may be calculated from

$$2 \ln \frac{X^{Sil}_{Al_2SiO_5}}{X^{And}_{Al_2SiO_5}} = -\frac{\Delta V}{RT}(P - P_0) \qquad (2)$$

using the molar volumes given in Table 6. Note that ln X values are doubled because two sites are involved. The one-site model would begin with $X_{FeAlSiO_5}$ twice as large as $X_{Fe_2SiO_5}$ and, without squaring, the two terms would be nearly equal at values of $X_{Al_2SiO_5}$ greater than about 0.95.

In each case, reactions involving Al_2SiO_5 in the Picuris rocks occurred with increasing T, that is Ky → Sil, Ky → And, or And → Sil. Any phase diagram representing reactions in the Picuris rocks must have P_f-T fields for both single- and two-phase occurrences. Kerrick and Speer (1988) illustrate the divariant field concept. However, in the rocks studied, saturation with hematite-ilmenite and quartz eliminates divariancy in the normal sense of the word. In a system that includes Al_2SiO_5, hematite-ilmenite, and quartz, the product Al_2SiO_5 phase would not return to the composition of the reactant Al_2SiO_5 polymorph as illustrated by Kerrick and Speer (1988, Fig. 3); rather both phases would remain saturated with Fe^{3+} for the particular hematite-ilmenite composition in the rock. Thus, for any given reactant composition, there is a single univariant P_f-T reaction line. Two-phase fields result from the fact that reactants and products have a range of composition between specimens, depending primarily on the amount of hematite component in the hematite-ilmenite. Two-phase assemblages in the Picuris rocks must result primarily from arrested reaction.

The P_f-T diagrams of Figure 4 were calculated to show the first and last reactions for each area. Rather than use the product analyses (Table 2) for these equilibrium calculations, we determined coexisting product compositions using our established K_n values (Table 5). This has the result in minimizing effects of disequilibrium composition and analytical error. In Reaction 1, for example, in Hondo Canyon, the first R1 andalusite to react would be $X_{Fe_2SiO_5} = 0.013$ (specimen 9, Table 2), and it would produce sillimanite with $X_{Fe_2SiO_5} = 0.0065$. Similarly, the last such reaction (specimens 4, 30, 10, 29, and 13) is andalusite (0.015) to sillimanite (0.0075).

Four pure Al_2SiO_5 diagrams are consistent with the chloritoid-staurolite equilibria discussed below. These are Holdaway (1971), Kerrick and Heninger (1984) as modified by Kerrick and Speer (1988), Helgeson et al. (1978), and Berman (1988). Triple-point conditions among these equilibrium diagrams range over approximately 300 bars and 20 °C. In order to construct a series of modified diagrams for Al_2SiO_5 polymorphs we have chosen the GeO-Calc program (Brown et al., 1988) and the Berman (1988) thermodynamic data because (1) they are based on both the Holdaway (1971) and Kerrick and Heninger (1984) experiments, and (2) they are an internally consistent data set resulting from analysis of the most recent thermodynamic data. The Fe-free triple point using the Berman (1988) data is 506 °C, 3.733 kbar.

Our modified Al_2SiO_5 diagrams for the two areas, calculated using GeO-Calc, are illustrated in Figure 4. When one keeps in mind the foregoing discussion and assumes minimum overstepping for initiation of reaction, several points are important for relating mineral assemblages to phase diagrams: (1) when an Al_2SiO_5 polymorph occurs by itself in a rock or unit, the P_f-T conditions must lie in the appropriate one-phase field, the boundaries of which are determined by a single set of P_f-T lines: (2) when two Al_2SiO_5 phases stably coexist in a rock, the P_f-T conditions lie on the appropriate P_f-T line; and (3) in any natural system, many specimens will not adhere to these simple rules, the most common deviation being the metastable preservation of a reactant with the product phase a few degrees into a product-phase field. The idea of minimal overstepping of silicate reactions is supported by the work of Wood and Walther (1983).

In Figure 4, dashed lines represent reactions in progress and solid lines bracket reactions that have not occurred or have gone to completion. For each, the value of $X_{Fe_2SiO_5}$ of the reacting phase, or bracketed phase, is given. The size of the boxes represents the estimated variation in P_f and T for each area, not the error. In Hondo Canyon, both Ortega and R1 show partial reaction to sillimanite in most specimens, but sillimanite formation is volumetrically much more extensive in Ortega than in R1. Figure 4a shows that, given the same T range, this is due to the wider spread of equilibrium curves for the reaction And → Sil. The only specimen that exhibits the reaction Ky → And (27, Table 2) contains the most Fe-rich reacting kyanite, and this stabilizes the triple point to higher P_f and T. The most Fe-rich nonfibrolitic sillimanite (specimen 1, Table 2) occurs in an Ortega specimen without kyanite, as would be expected. The positioning of the P_f-T boxes in Figure 4a reflects metastable preservation of some reacting andalusite or kyanite 1–2° into the sillimanite field (consistent with values suggested by Wood and Walther, 1983).

The data for Section 8 do not constrain conditions as well as those for Hondo Canyon. The absence of sillimanite from all but two Ortega specimens and the lower Fe content of kyanite reacting initially to andalusite indicate lower P_f and T. The Ortega conditions are well

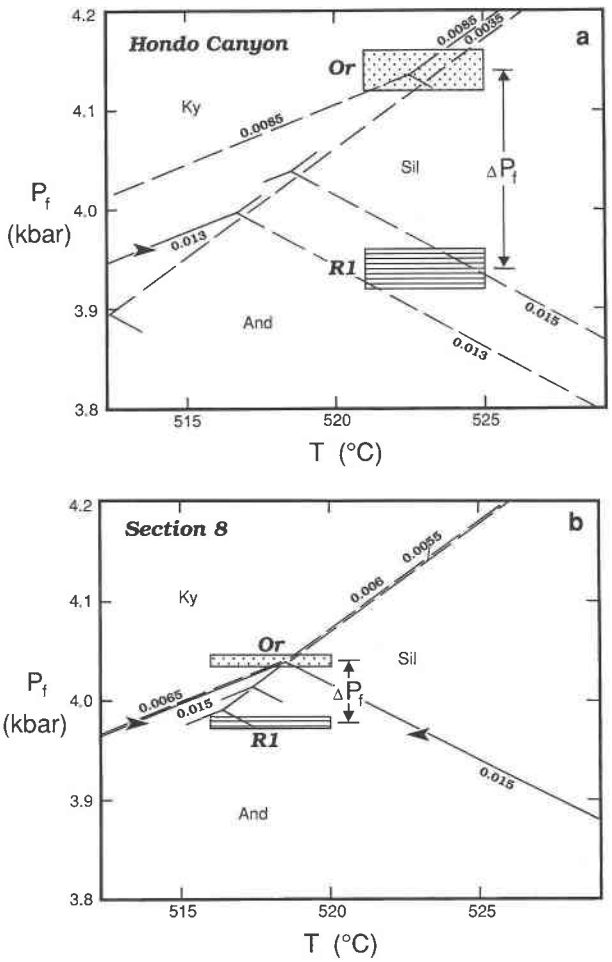

Fig. 4. P_f-T plots of the Al_2SiO_5 triple-point region for the Hondo Canyon (**a**) and Section 8 (**b**) areas, illustrating conditions of formation for Ortega quartzite (Or) and R1 units based on occurrence and composition of Al_2SiO_5 polymorphs. Long dashed lines give the conditions for coexisting Al_2SiO_5 pairs. Solid lines show bracketing reactions deduced from a one-phase equilibrium with arrows pointing to the observed phase for a given unit. Numbers refer to X_{Fe} in reacting andalusite or kyanite, or, for bracketing reactions, X_{Fe} in the observed phase (fourth-place figures for reactant compositions are not considered significant, but show the values that have been halved from measured product compositions). The Fe-free triple point is at 506 °C, 3.733 kbar. Boxes represent estimated ranges of conditions within Ortega (dotted) and R1 (ruled). Temperature variation in each unit is assumed to be 4 °C, and the units are considered to be under isothermal conditions. Note that in both areas the most Fe-rich Ortega kyanite has begun reacting to andalusite, thus helping to constrain the Ortega conditions. Pressure difference between units (ΔP_f) in the Hondo Canyon area (a) is deduced to be 200 bars, in order to satisfy constraints of triple-point assemblage in Ortega and the reaction And → Sil in R1. In the Section 8 area (b), ΔP_f is constrained to be a minimum of 50 bars, but may be greater because R1 only contains andalusite and lower pressures are permissive. Similar petrographic and compositional constraints within the two areas indicate that the value of 200 bars for the Hondo Canyon area may be the best estimate of ΔP_f for each area.

constrained near the triple point for kyanite with $X_{Fe_2SiO_5} = 0.0065$. The R1 rocks, containing only andalusite, must have equilibrated at T above the kyanite field and below the sillimanite field. The precise P_f cannot be determined, but it is at least 50 bars below that for Ortega. The primary reason that the rocks of Section 8 do not constrain ΔP_f very well is that they represent more restricted ranges of kyanite composition in Ortega and andalusite composition in Rinconada than for the Hondo Canyon occurrence.

One possible method of rationalizing the apparent difference in P_f between Ortega and Rinconada rocks is to infer that certain phases did not form because of overstepping of equilibrium curves. By this scenario, it might be argued that equilibrium andalusite formation was somehow inhibited in most Ortega rocks and that sillimanite in these rocks formed by reaction of kyanite on or above the metastable extension of the kyanite-sillimanite equilibrium curve. A strong argument against this possibility is the fact that in the three instances where andalusite did form from Ortega kyanite, the kyanite was the most Fe-rich kyanite in the area (Table 2). This indicates that (1) the andalusite was stabilized to its highest possible pressures in such rocks (Fig. 4), (2) this andalusite formed with minimal overstepping, and (3) avoidance of andalusite by reaction of kyanite with less Fe would require substantially more overstepping. In addition, the overall regularity of compositional behavior of the minerals argues against significant amounts of overstepping or inhibition of equilibrium formation of polymorphs.

Yet another potential explanation for apparent differences in P_f between the units is the small differences in f_{O_2} between the units. As demonstrated above, average f_{O_2} in Ortega was slightly higher than that of R1. Because andalusite contains the most Fe_2O_3 of the Al_2SiO_5 polymorphs, it should be stabilized by elevated f_{O_2}. In fact the reverse is true, and Ortega contains less andalusite than R1.

Thus, we conclude that equilibria involving Al_2SiO_5, when corrected for dilute Fe contents of the polymorphs, reflect real differences in P_f between the Ortega and R1 units. The difference in P_f between these nearly adjacent units (ΔP_f) is about 200 ± 100 bars in Hondo Canyon, but it is less well defined in Section 8. Our method of estimating error in ΔP_f is discussed below.

Chloritoid-staurolite equilibria

With a single exception, discussed below, chloritoid is restricted to Ortega rocks, and staurolite is restricted to Rinconada rocks. At first glance, it would appear that this observation provides evidence for higher P_f in the Ortega unit, given constant T. However, staurolite in the Rinconada Formation is more Mg-rich and contains less H than staurolite that would be produced from reaction of the Ortega chloritoid (Tables 3, 4). Accordingly the occurrence of staurolite in Rinconada rocks and chloritoid in Ortega rocks does not require any difference in intensive variables between the units. We discuss the occurrences in order to show (1) that Holdaway (1978) was incorrect in suggesting that Rinconada staurolite required lower P_{H_2O} than Ortega chloritoid and (2) that the chloritoid and staurolite occurrences permit acceptance of the ΔP_f value estimated for the Hondo Canyon Al_2SiO_5 phases. We emphasize that this discussion, involving hypothetical compositions of Ortega staurolite and Rinconada chloritoid, is an approximate treatment that has significant error, as discussed in a later section. However, we believe that the discussion adds to our understanding of these complex relationships.

Some combination of the following three equilibria, shown as Fe end-member reactions, is mainly responsible for the stability of staurolite in Rinconada R0 and R1 rocks. We note that for none of these reactions do we find both reactants and products present in the same unit. Thus the reactions can only bracket P_f-T conditions.

$$\underset{\text{Chloritoid}}{Fe_2Al_4Si_2O_{10}(OH)_4} + 2.716\ \underset{\text{And, Ky, Sil}}{Al_2SiO_5} = 0.5263\ \underset{\text{Staurolite}}{H_4Fe_{3.8}Al_{17.92}Si_{7.66}O_{48}} + 0.685\ \underset{\text{Quartz}}{SiO_2} + 0.947\ \underset{\text{Fluid}}{H_2O} \quad (3)$$

$$\underset{\text{Chloritoid}}{Fe_2Al_4Si_2O_{10}(OH)_4} + 0.632\ \underset{\text{Quartz}}{SiO_2} = 0.1752\ \underset{\text{Staurolite}}{H_{3.5}Fe_{4.05}Al_{17.92}Si_{7.66}O_{48}} + 0.438\ \underset{\text{Garnet}}{Fe_3Al_2Si_4O_{12}} + 1.693\ \underset{\text{Fluid}}{H_2O} \quad (4)$$

$$\underset{\text{Chloritoid}}{Fe_2Al_4Si_2O_{10}(OH)_4} + 0.299\ \underset{\text{Muscovite}}{KAl_3Si_3O_{10}(OH)_2} = 0.2566\ \underset{\text{Staurolite}}{H_3Fe_{4.3}Al_{17.92}Si_{7.66}O_{48}} + 0.299\ \underset{\text{Biotite}}{KFe_3AlSi_3O_{10}(OH)_2} + 0.034\ \underset{\text{Quartz}}{SiO_2} + 1.615\ \underset{\text{Fluid}}{H_2O} \quad (5)$$

Additional staurolite-forming reactions may be written using chlorite with or without garnet as a reactant. Such reactions would apply to R2; however, R0 bulk composition lies entirely above the garnet-chlorite join in AFM projection, and R1 bulk composition lies largely above the garnet-chlorite join. For rocks of such aluminous compositions, chloritoid must precede staurolite (Albee, 1972). All biotite in R0 and R1 is randomly oriented and is interpreted to have grown near the thermal peak of metamorphism from the reaction of staurolite and chlorite. Regardless of which reaction actually produced the staurolite in R0 and R1, the existence of product assemblages for Reactions 3, 4, and 5, combined with appro-

priate activity corrections, establishes that the products formed at T above the reaction boundary.

The reactions are listed in probable order of increasing T (or decreasing P_f) for the Fe end-members. However, fractionation of Mn into garnet and Mg into biotite (Holdaway, 1978; Goodge and Holdaway, unpublished data) lowers the T of Reaction 4 in R1 and Reaction 5 in R0 and R1, whereas these compositional effects do not significantly change Reaction 3. Thus it is possible that all three reactions may have proceeded nearly simultaneously in Rinconada R0 and R1. For Ortega quartzite the low-T sides of all three reactions were stable, for R0 the high-T sides of Reactions 3 and 5 were stable, and for R1 the high-T sides of all three reactions were stable.

Staurolite formulas given above are based on the work of Holdaway et al. (1986a, 1988), and reflect a vacancy-vacancy substitution of H for R^{2+}. Holdaway et al. (1986a, 1986b) showed that staurolite that forms with biotite or garnet has about three H, whereas that which forms in the absence of biotite or garnet has about four H. The high-H staurolite often coexists with chloritoid. The staurolite composition for Reaction 4 is assumed to be intermediate (H $\approx$ 3.5) because chloritoid and garnet together should buffer staurolite R^{2+} at intermediate values.

The best reaction to study in detail to compare intensive variables in Ortega and Rinconada rocks is Reaction 3 applied to Ortega and R0 for the following reasons: (1) none of the participating phases varies more than 20 mol% from Fe end-member compositions; (2) the P_f-T location of the end-member reaction is reasonably well known; and (3) the composition of the staurolite reaction product is reasonably well known. Reactions 4 and 5 would give comparable results with considerably larger errors. Because R0 is restricted to Hondo Canyon, the calculations apply only to this area, but the similarity of the other Section 8 assemblages to those of Hondo Canyon implies that conclusions based on R0 may also be applied to Section 8.

For our calculations, several assumptions were necessary to determine the compositions of hypothetical staurolite in Ortega and chloritoid in R0. These assumptions have a bearing on the error of the calculations, as discussed below. (1) Li content of all staurolite, actual and hypothetical, was set at 0.2 atoms pfu. This is a reasonable average for both pelites and quartzites (Dutrow et al., 1986). (2) Zn content of hypothetical staurolite in Ortega quartzites was set at 0.02 atoms pfu, consistent with the low Zn of the staurolite in adjacent R0. (3) Ti content of hypothetical Ortega staurolite was set as 0.1, consistent with Ti in R0 staurolite. (4) K_D for staurolite Fe/Mn over chloritoid Fe/Mn was set at one (Albee, 1972). (5) K_D for staurolite Fe/Mg over chloritoid Fe/Mg was set at values given by Grambling (1983, Fig 10) for staurolite with Mg/(Mg + Fe) < 0.10 and at 1.2 for more Mg-rich staurolites (Albee, 1972). (6) Analyzed staurolites in R0 were assumed to have three H, consistent with available Picuris data (Table 4), and data for staurolites in other biotite-bearing, chloritoid-absent rocks (Holdaway et al., 1986a). Hypothetical staurolites in the Ortega were assumed to have four H, because they would have formed with chloritoid in the absence of biotite or garnet. In order to accomplish this, the total R^{2+} + Li + Ti was normalized to 4.3 atoms (0.1 tetrahedral vacancy) in R0, and 3.8 atoms (0.6 tetrahedral vacancy) in hypothetical Ortega staurolite. (7) Effects of oxidizing conditions were ignored, because we have no accurate information on the Fe^{3+} content of either chloritoid or staurolite. Fe^{3+} probably replaces Al to some degree in all phases of Reaction 3, such that dilution effects tend to cancel each other.

TABLE 7. ΔV and ΔS for Reaction 3 at 800 K

Al_2SiO_5 mineral	P(kbar)	ΔV(J/bar)	ΔS(J/K)	dP/dT(bar/K)
Kyanite	4.4	1.124	105.11	93.5
Sillimanite	4.0	−0.379	73.78	−194.7
Andalusite	3.8	−0.796	82.17	−103.2

Note: Thermal expansion and compressibility of solids are ignored. These effects tend to cancel out for the reaction. Data from Table 6.

Over small T intervals, the offset ($T - T_0$) from the pure end-member curve for Reaction 3 (Richardson, 1968) to limiting curves for Ortega and R0 rocks may be calculated from

$$0.5263 \ln a^{St} - \ln a^{Cld} = \frac{\Delta S}{RT}(T - T_0). \qquad (6)$$

Entropy (ΔS, Table 7) was evaluated near the midpoint of the T offset using data given in Table 6. Chloritoid solid solution is assumed to be ideal and thus has an activity model of X^2_{Fe}. The activity model for staurolite in Reaction 3, based on Holdaway et al. (1988), is

$$\frac{{}^{[4]}X^{3.4}_{Fe} \times {}^{[4]}X^{0.6}_{\square} \times {}^{[u]}X^{0.25}_{Fe} \times {}^{[u]}X^{1.75}_{\square,i}}{{}^{[4]}X^{3.4}_{Fe,i} \times {}^{[4]}X^{0.6}_{\square,i} \times {}^{[u]}X^{0.25}_{Fe,i} \times {}^{[u]}X^{1.75}_{\square,i}} = 9.122 \times {}^{[4]}X^{3.4}_{Fe} \times {}^{[4]}X^{0.6}_{\square} \times {}^{[u]}X^{0.25}_{Fe}. \qquad (7)$$

A constant, 0.15Fe, was assigned to Al(3A) sites in both end-member and natural staurolite, and 0.25(Mn + Fe) was split between two U sites, leaving the remaining Fe and all Mg, Zn, Li, Ti, and vacancies to total four for the tetrahedral Fe sites.

The initial T for end-member Reaction 3 was chosen to be 545 °C at 4.7 kbar, consistent with the experimental results of Richardson (1968), and with the Al_2SiO_5 phase diagram corrected for Fe^{3+} (Fig. 5). Values of $T - T_0$ for Ortega and R0 at 4 kbar with sillimanite are 21 ± 2 °C and 36 ± 1 °C (1σ), respectively. In Figure 5, the T range (ΔT) over which Ortega and R0 could have formed at the same T varies from 10 to 14 °C in width in the P_f range indicated for Hondo Canyon Ortega and R0.

The P_f-T boxes in Figure 5 are represented as determined in Figure 4a. The lines for Reaction 3 are very steep, as indicated by dP/dT calculated from ΔS and ΔV (Table 7). In the sillimanite and uppermost andalusite

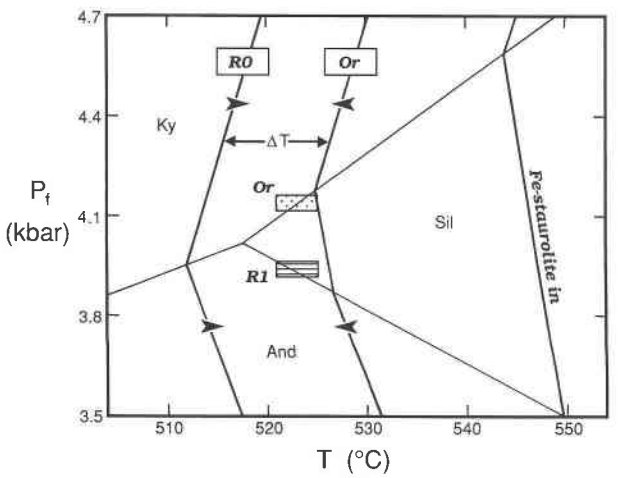

Fig. 5. End-member equilibrium curve (far right) and bracketing equilibrium curves for Reaction 3 applied to Hondo Canyon R0 and Ortega (Or). The calculated curves are based on compositions of existing R0 products and Ortega reactants and calculated hypothetical R0 reactants and Ortega products. Arrows indicate on which side of the reaction curve each unit should lie. Light lines give average Al_2SiO_5 stability relations based on Figure 4a. The separation between the R0 and Ortega curves, indicated by ΔT, shows the interval in which both rock types can exist at the same T. Boxes show ranges of conditions for Ortega and R1 taken from Figure 4a and illustrate that the chloritoid-staurolite equilibria permit differences in P_f between Ortega and Rinconada.

fields, the curves actually have negative slopes, required by negative ΔV values. Ortega chloritoid compositions would react to staurolite above the peak T of metamorphism, and R0 staurolites formed at lower T from the reaction of chloritoid and other phases. The difference in T of the reaction for the two occurrences results primarily from two related factors: the more Mg-rich composition, and the higher R^{2+} (fewer tetrahedral vacancies) of Rinconada staurolite than of the hypothetical Ortega staurolite. The more Mg-rich composition favored complete destruction of chloritoid by Reaction 5. With chloritoid gone and biotite present, staurolite composition attained higher tetrahedral occupancy and lower tetrahedral vacancies, and thus a lower activity of the end-member staurolite shown for Reaction 3. The fact that chloritoid in R0 was destroyed by Reaction 5 has no direct bearing on the fact that the R0 assemblage may be shown to have occurred above conditions for Reaction 3 (Fig. 5), as long as the proper activity corrections are made.

Another possible explanation for the difference in the occurrence of chloritoid and staurolite between the Ortega and Rinconada rocks is the difference in average f_{O_2} between units. Ganguly (1969) has shown experimentally that Reaction 3 proceeds at higher T under oxidizing conditions than under reducing conditions. This is probably not the most important reason for the difference in occurrence because the range of f_{O_2} in Ortega, R0, and R1 is restricted by the hematite-ilmenite miscibility gap, and individual occurrences in each unit overlap the others in f_{O_2}.

The chloritoid-staurolite calculations permit, but do not require, P_f to be different for Ortega and Rinconada rocks. The following points summarize our interpretation of phase relations. Among Al_2SiO_5 polymorphs at uniform T, Rinconada andalusite in Hondo Canyon formed at P_f about 200 bars lower than Ortega kyanite (both of which partially reacted to form sillimanite); in Section 8 the andalusite also formed at lower P_f than the kyanite (minimum difference of about 50 bars). From chloritoid-staurolite equilibria in the Hondo Canyon sequence, Ortega chloritoid and Rinconada staurolite could have formed under identical P_f-T conditions, but the steep curves of Figure 5 permit Rinconada P_f to be lower than that for Ortega.

One staurolite analysis requires separate discussion, that of Ortega specimen 25 (Table 4). This low-Mg staurolite occurs as a few grains along a pelitic horizon in the quartzite along with Fe-rich chloritoid and kyanite. The microprobe analysis showed a low total oxide content, anomalously high Al_2O_3, and very low R^{2+}. The sum of H and Li, calculated on the basis of Si + Al = 25.53, is 6.547. These anomalies suggested that the staurolite probably contains high Li (Dutrow et al., 1986). The microprobe section was sent to Richard Hervig at Arizona State University for analysis of Li and H by ion probe. The results were H_2O = 2.1 wt%, Li_2O = 1.42 wt% (Table 4). The 1.566 Li atoms pfu represent the highest known Li content in a natural staurolite. The 3.843 H atoms pfu are slightly lower than expected for a staurolite occurring with chloritoid (see above). This is probably explained by the fact that saturation or near-saturation in one non-Fe tetrahedral component (Li) tends to reduce the amount of other non-Fe tetrahedral components (Mg, tetrahedral vacancies) as shown by Holdaway et al. (1988) for Li and Mg. The very high Li stabilized staurolite to lower temperatures, explaining why it occurs in a unit that otherwise has no staurolite.

Discussion of error

In calculations of this type it is very difficult to realistically assess error. Error comes from four unrelated sources: (1) experimental calibration of equilibrium curves; (2) error in the P or T offsets that results from analytical error and error in determination of ΔV and ΔS; (3) error in the P or T offsets that results from assumed compositions of hypothetical staurolite or chloritoid; and (4) error in the P or T offsets that results from actual nonideality when ideality is assumed.

For reactions among Al_2SiO_5 polymorphs and Reaction 3, realistic errors for the experimental equilibrium curves are 25 °C and 0.25 kbar. These errors are somewhat smaller than those estimated for the original experiments, but these estimates appear warranted on the basis of the very good consistency among the various diagrams cited above and the Richardson (1968) chloritoid-staurolite experiments (Fig. 5). For the most part, these errors need

not enter into the discussion of the error in ΔP_f (Fig. 4a) and ΔT (Fig. 5) because the experimental calibrations affect end-member equilibrium curves for both units to a similar extent. However, this error of experimental calibration may help to explain the small apparent differences between the average results of garnet-biotite geothermometry (532 °C) and the average results based on Al_2SiO_5 occurrence and composition (523 °C, Fig. 4a) for Hondo Canyon.

For the error in ΔP_f, based on Al_2SiO_5 reactions illustrated in Figure 4, errors related to analytical precision and the value of ΔV are small. Error involved in the assumption of ideal solid solution is also small because of the low concentrations of Fe^{3+} and the fact that such assumptions affect the two units similarly. The main sources of error are the positioning of the P_f-T boxes and the slope of the andalusite-sillimanite boundary. Experimentation with different Al_2SiO_5 equilibria, various values for T range, and various positions for the boxes suggests that an error of 100 bars in the 200-bar value of ΔP_f is realistic.

For Reaction 3 the potential sources of error are greater. ΔV is reasonably accurate and has an important effect on the slopes of the curves, causing a slope reversal at the edge of the kyanite field (Fig. 5). Error due to analytical uncertainties is negligible, but the error from assuming H_2O content of the staurolites is significant. There appear to be three important sources of error, as follows. (1) The error in assumed average H content of staurolite is related to the difference in H between R0 and hypothetical Ortega staurolite. This difference could conceivably be as low as 0.75 or as high as 1.25, instead of 1. (2) The error in ΔS is estimated to be 25%. (3) Error in the assumption of ideality in staurolite tetrahedral Fe sites is also possible. There is a very real probability of nonideality as suggested by Holdaway et al. (1988). A reasonable model for this nonideality is a pseudobinary solid solution with Fe as one component and Mg, Li, Zn, Ti, and tetrahedral vacancies as the other. Holdaway et al. (1988) assumed the vacancies behaved ideally. For a trivial content of tetrahedral vacancies, this approach was satisfactory. Because there appears to be a limiting value for each component except Fe, it appears reasonable to group them as the other pseudobinary component in Fe-rich staurolites. If this approach is valid, then nonideality tends to cancel out for the present situation. End-member staurolite for Reaction 3 contains about 15% non-Fe tetrahedral component, R0 staurolite contains about 28%, and hypothetical Ortega staurolite contains about 29%. Nonideality would reduce somewhat the value of $T - T_0$, because of the greater amount of non-Fe components in the natural staurolites, but the effect would be about the same in both units.

Overall, we estimate a 50% error in $T - T_0$ for each unit. At 4 kbar, and with the appropriate stable form of Al_2SiO_5, the T offsets (Fig. 5) have estimated minimum and maximum limiting values, respectively $(T - T_0)_{min}$ and $(T - T_0)_{max}$, as follows: (1) for R0, 17° and 52°; and (2) for Ortega, 11° and 32°. Most aspects of the error affect $T - T_0$ to the same extent for both units. Thus ΔT at 4 kbar, which is 14° in Figure 5, could be as low as 6° or as high as 20°. In any event, there is sufficient space and the curves are steep enough to allow Ortega chloritoid-kyanite and R0 staurolite to be at the same T and different P_f.

Discussion

There may be some debate regarding the magnitude of ΔP_f, but there is little doubt that there was a small but real difference in intensive variables during metamorphism between the Ortega and Rinconada units, as exemplified by the presence of andalusite in Rinconada and kyanite in Ortega rocks. This relationship occurs all along the north flank of the Picuris Range and has been carefully studied at two localities. Specimens of andalusite-bearing Rinconada occur as close as 35 m from kyanite-bearing Ortega in map view (Fig. 3), and as close as 20 m stratigraphically (Table 2).

Oxygen fugacity and T can be ruled out as critical variables; hematite-ilmenites and Al_2SiO_5 phases have comparable Fe^{3+} contents between units, and the thicknesses of and distances between the units are too small for any significant T differences to have existed. Similarly, P_r cannot have varied between the units because they have similar elevations (Figs. 2, 3; Table 2), and, by extension, similar depths during metamorphism. The minerals involved are anhydrous; thus differences in X_{H_2O} cannot account for the different mineral occurrences.

The only intensive variable remaining that could vary over such short distances and yet be stratigraphically controlled is P_f. From both solid-solid and solid-fluid equilibria we estimate the difference in fluid pressure (ΔP_f) between the Ortega and Rinconada units to be approximately 200 ± 100 bars. This estimate of ΔP_f is of the same order of magnitude as was estimated by Bruton and Helgeson (1983) for fluid pressure variation over a vertical distance of 1 km in metamorphic or hydrothermal systems, which under conditions of $P_f = P_r$ is estimated to be 200–300 bars km^{-1}, and under conditions of $P_f < P_r$ is estimated to be about 100 bars km^{-1}. Because the stratigraphic differences between the Ortega and Rinconada units are much less than 1 km, and premetamorphic folding probably eliminated this small amount, the ΔP_f we estimate in this case probably depends on differences in rock permeability.

Consideration of a model for fluid transport in metamorphic rocks by Walther and Orville (1982) appears to require that P_f be approximately equal to P_r in rocks with tightly arranged grain boundaries, such as the Ortega quartzites. In rocks of this type, fluids trapped in isolated fractures would in fact have to be at $P_f \geq P_r$ for the fractures to remain open and propagate upward. By similar reasoning, the ΔP_f observed between the Ortega and Rinconada units (in which both were at identical P_r) suggests that for the Rinconada schists $P_f < P_r$. This situation appears to be possible only when fluids are allowed to

migrate along planar grain-boundary channels subparallel to foliation rather than along newly opened fractures that form only when P_f exceeds P_r. However, Walther and Orville (1982) also argue that because the tensile strength of micaceous pelites is very small under midcrustal conditions, an evolved fluid will be able more easily to fracture the rock, mostly along existing foliation planes, and escape upward owing to its lower density. Thus, a difference in rock permeability appears to be the dominant control on effective pressure.

Support for our inferences of a permeability contrast between rock units comes from a theoretical study of rock porosity by Walder and Nur (1984), who concluded from their mathematical models that elevation in P_f is dependent on porosity reduction, which in general reduces permeability. However, Watson and Brenan (1987) observed formation of moderate pore connectivity (implying finite porosity and permeability) in experimentally annealed quartzites containing high-X_{H_2O} fluids. Although we concur that quartz-rich rocks such as the Ortega quartzites may undergo an increase in such pore connectivity from infiltrating aqueous fluids, we infer from our results that permeability in such rocks should remain lower than that in coarsely recrystallized mica schists.

Because the difference between chloritoid + kyanite in Ortega and staurolite in R0 can be explained by bulk composition alone, it is not necessary that P_f change abruptly at the Ortega-Rinconada contact. In Hondo Canyon, P_f decreased by as much as 200 bars over a stratigraphic distance of approximately 25 m between Ortega and R1. Although not as well documented, a similar change may have occurred within a covered interval in Section 8 of no more than 20 m stratigraphically. The R0 rocks contain more mica than Ortega and less than R1 (Table 1). Thus it appears reasonable that there is a rough correlation between P_f and mica content. Once the rocks developed a highly micaceous character and a pervasive schistosity, P_f reached but could not surpass a finite maximum value inferred for Rinconada schists.

We infer that the decrease in P_f from Ortega to R1 was facilitated by a large increase in muscovite content between units from 1–3% up to 30–50%. The oriented mica with its planar boundaries provided a faster escape for fluids along foliation planes than the granular and interlocking quartz. Thus the effective permeability was greater in the schists than in the quartzites. The value of ΔP_f is about 5% of the total P_f in the quartzites. A drop from lithostatic to hydrostatic fluid pressure would represent a 65% decrease in P_f, so that the 5% actual P_f decrease was about 8% of the total possible P_f decrease from lithostatic to hydrostatic. Such a change could easily have been facilitated by a difference in permeability between rock types. Our conclusions from this analysis are corroborated by petrologic and stable-isotope evidence for limited channelized fluid flow in which the Ortega and Rinconada units maintain unique fluid compositions (Goodge and Holdaway, unpublished data).

The hypothesis of a difference in an intensive variable between Ortega and Rinconada rocks and the likelihood that this difference is in P_f provide a strong supporting case for the Bruton and Helgeson (1983) model that P_f is the effective pressure on all solids when a fluid phase is present. The significance of this conclusion is that petrologists should be careful in interpreting the meaning of the effective pressure on solids. Several important points come to mind: (1) Most metamorphic processes take place in a fluid-present system; therefore, when one determines P from solid mineral equilibria, this pressure is P_f, not P_r. (2) This effective pressure is the rigorous sum of the fluid partial pressures, not the approximate sum. (3) P_f may vary locally, especially between rock types as physically different as quartzites and schists. (4) There is no absolute correlation between P_f and depth of overburden (or lithostatic pressure, P_r). However, low-permeability rocks may have formed under conditions of P_f approaching P_r. Certainly, one must keep in mind the possibility that the effective pressure on schists may be 100–200 bars lower than the effective pressure on neighboring quartzites.

The present observations may not extend to metamorphism at high grades where melt is locally generated and fluid-producing reactions are less common. If the fluid-pressure sum was low enough that no fluid phase was present at all, a different approach may be necessary. The Bruton and Helgeson (1983) approach is best applied to the study of progressive metamorphism in low- to medium-grade terranes where fluid components were abundant. Differences in P_f between adjacent units may only be significant where contrasts between permeabilities are high, such as in quartzite-schist or pelite-carbonate transitions.

Conclusions

1. Mineralogic differences between rock units on the northern flank of the Picuris Range are directly or indirectly the result of stratigraphic (i.e., compositional) differences.

2. The occurrence of kyanite ± sillimanite in the Ortega quartzites overlain by andalusite ± sillimanite in the Rinconada schists might well be explained by differences in P_f.

3. The occurrence of chloritoid + kyanite in the Ortega and staurolite in the Rinconada can be explained by more Mg-rich rock compositions with lower H and higher total R^{2+} in Rinconada staurolite than would have formed in Ortega. The more Mg-rich rock compositions aided a reaction that consumed chloritoid in the presence of muscovite. Steep chloritoid reaction boundaries permit, but do not require, differences in P_f between the units.

4. The difference in P_f between the units probably results from greater effective permeability in the most micaceous rocks. Because it is difficult to explain the mineralogic differences with P_r, these observations provide support for the Bruton and Helgeson (1983) model that P_f is the effective pressure on solid minerals during metamorphism.

5. Petrologists should be careful to note that total pressure measured in low- and medium-grade metamorphic terranes is probably P_f in the presence of fluids and that it is not directly correlated with overburden depth, but rather may vary slightly between rock types.

Acknowledgments

We wish to acknowledge the assistance of Dwight Deuring with the microprobe and Biswajit Mukhopadhyay with computer work. Sample collection and mapping was done mainly by Cheryl Rattel-Carson. The GeO-Calc program and related advice were provided by R.G. Berman (University of British Columbia and the Canadian Geological Survey). Ion probe analysis of light elements on specimen 25 was kindly provided by Richard Hervig (Arizona State University). We thank these people for their valuable help. Jeff Grambling, Hal Helgeson, and Mark Helper provided thoughtful reviews of the manuscript, but the interpretations presented in this paper remain strictly our own. The research was supported by NSF grants EAR-8606489 and EAR-8904777.

References cited

Albee, A.L. (1972) Metamorphism of pelitic schists: Reaction relations of chloritoid and staurolite. Geological Society of America Bulletin, 83, 3249–3268.

Bauer, P.W. (1984) Stratigraphic summary and structural problems of Precambrian rocks, Picuris Range, New Mexico. In W.S. Baldridge, P.W. Dickerson, R.E. Riecker, and J. Zidek, Eds., Rio Grande Rift: Northern New Mexico, New Mexico Geological Society guidebook, 35th field conference, 199–204.

Bauer, P.W., and Williams, M.L. (1989) Stratigraphic nomenclature of Proterozoic rocks, northern New Mexico—Revisions, redefinitions, and formalization. New Mexico Geology, 11, 45–52.

Bayly, Brian (1987) Nonhydrostatic thermodynamics in deforming rocks. Canadian Journal of Earth Sciences, 24, 572–579.

Berman, R.G. (1988) Internally-consistent thermodynamic data for minerals in the system Na_2O-K_2O-CaO-MgO-FeO-Fe_2O_3-Al_2O_3-SiO_2-TiO_2-H_2O-CO_2. Journal of Petrology, 29, 445–522.

Brace, W.F. (1980) Permeability of crystalline and argillaceous rocks. International Journal of Rock Mechanics Mineral Science, 17, 241–251.

Brown, T.H., Berman, R.G., and Perkins, E.H. (1988) GeO-Calc: Software package for calculation and display of pressure-temperature-composition phase diagrams using an IBM or compatible computer. Computers and Geosciences, 14, 279–289.

Bruton, C.J., and Helgeson, H.C. (1983) Calculation of the chemical and thermodynamic consequences of differences between fluid and geostatic pressure in hydrothermal systems. American Journal of Science, 283-A, 540–588.

Burnham, C.W., Holloway, J.R., and Davis, N.F. (1969) Thermodynamic properties of water to 1,000 °C and 10,000 bars. Geological Society of America Special Paper 132.

Dickerson, R.P., and Holdaway, M.J. (1989) Acadian metamorphism associated with the Lexington batholith, Bingham, Maine. American Journal of Science, 289, 945–974.

Dutrow, B.L., Holdaway, M.J., and Hinton, R.W. (1986) Lithium in staurolite and its petrologic significance. Contributions to Mineralogy and Petrology, 94, 496–506.

Etheridge, M.A., Wall, V.J., Cox, S.F., and Vernon, R.H. (1984) High fluid pressures during regional metamorphism and deformation: Implications for mass transport and deformation mechanisms. Journal of Geophysical Research, 89, 4344–4358.

Fyfe, W.S., Price, N.J., and Thompson, A.B. (1978) Fluids in the Earth's crust. Elsevier, New York.

Ganguly, J. (1969) Chloritoid stability and related parageneses: Theory, experiments, and applications. American Journal of Science, 267, 910–944.

Ganguly, J., and Newton, R.C. (1968) Thermal stability of chloritoid at high pressure and relatively high oxygen fugacity. Journal of Petrology, 9, 444–466.

Ganguly, J., and Saxena, S.K. (1984) Mixing properties of aluminosilicate garnets: Constraints from natural and experimental data, and applications to geothermobarometry. American Mineralogist, 69, 88–97.

Gibbs, J.W. (1878) On the equilibrium of heterogeneous substances. Connecticut Academy Transactions, 3, 343–524.

Grambling, J.A. (1981) Kyanite, andalusite, sillimanite, and related mineral assemblages in the Truchas Peaks region, New Mexico. American Mineralogist, 66, 702–722.

——— (1983) Reversals in Fe-Mg partitioning between chloritoid and staurolite. American Mineralogist, 68, 373–388.

——— (1986) A regional gradient in the composition of metamorphic fluids in pelitic schist, Pecos Baldy, New Mexico. Contributions to Mineralogy and Petrology, 94, 149–164.

——— (1988) A summary of Proterozoic metamorphism in northern and central New Mexico: The regional development of 520 °C, 4-kb rocks. In W.G. Ernst, Ed., Metamorphism and crustal evolution of the western United States, Rubey vol. 7, p. 446–465. Prentice-Hall, Englewood Cliffs, New Jersey.

Grambling, J.A., and Williams, M.L. (1985) The effects of Fe^{3+} and Mn^{3+} on aluminum silicate phase relations in north-central New Mexico, U.S.A. Journal of Petrology, 26, 324–354.

Grew, E.S. (1980) Sillimanite and ilmenite from high-grade metamorphic rocks of Antarctica and other areas. Journal of Petrology, 21, 39–68.

Helgeson, H.C., Delany, J.M., Nesbitt, H.W., and Bird, D.K. (1978) Summary and critique of the thermodynamic properties of rock-forming minerals. American Journal of Science, 278A.

Hemingway, B.S., and Robie, R.A. (1984) Heat capacity and thermodynamic functions for gehlenite and staurolite: With comments on the Schottky anomaly in the heat capacity of staurolite. American Mineralogist, 69, 307–318.

Holdaway, M.J. (1971) Stability of andalusite and the aluminum silicate phase diagram. American Journal of Science, 271, 97–131.

——— (1978) Significance of chloritoid-bearing and staurolite-bearing rocks in the Picuris Range, New Mexico. Geological Society of America Bulletin, 89, 1404–1414.

Holdaway, M.J., Dutrow, B.L., and Shore, P. (1986a) A model for the crystal chemistry of staurolite. American Mineralogist, 71, 1142–1159.

Holdaway, M.J., Dutrow, B.L., Borthwick, J., Shore, P., Harmon, R.S., and Hintin, R.W. (1986b) H content of staurolite as determined by H extraction line and ion microprobe. American Mineralogist, 71, 1135–1141.

Holdaway, M.J., Dutrow, B.L., and Hinton, R.W. (1988) Devonian and Carboniferous metamorphism in west-central Maine: The muscovite-almandine geobarometer and the staurolite problem revisited. American Mineralogist, 73, 20–47.

Kamb, W.B. (1961) The thermodynamic theory of nonhydrostatically stressed solids. Journal of Geophysical Research, 66, 259–271.

Kerrick, D.M., and Heninger, S.G. (1984) The andalusite-sillimanite equilibrium revisited. Geological Society of America Abstracts with Programs, 16, 558.

Kerrick, D.M., and Speer, J.A. (1988) The role of minor element solid solution on the andalusite-sillimanite equilibrium in metapelites and peraluminous granitoids. American Journal of Science, 288, 152–192.

Kretz, R. (1983) Symbols for rock-forming minerals. American Mineralogist, 68, 277–279.

MacDonald, G.J.F. (1957) Thermodynamics of solids under non-hydrostatic stress with geologic applications. American Journal of Science, 255, 266–281.

Montgomery, A. (1953) Precambrian geology of the Picuris Range, north-central New Mexico. New Mexico Bureau of Mines and Mineral Resources Bulletin, 30.

Nielsen, K.C. (1972) Structural evolution of the Picuris Mountains, New Mexico. M.S. thesis, University of North Carolina, Chapel Hill, North Carolina.

Norris, R.J., and Henley, R.W. (1976) Dewatering of a metamorphic pile. Geology, 4, 333–336.

Ohmoto, H., and Kerrick, D.M. (1977) Devolatilization equilibria in graphitic systems. American Journal of Science, 277, 1013–1044.

Richardson, S.W. (1968) Staurolite stability in a part of the system Fe-Al-Si-O-H. Journal of Petrology, 9, 467–488.

Rumble, D., III (1978) Mineralogy, petrology, and oxygen isotope geo-

chemistry of the Clough Formation, Black Mountain, western New Hampshire, U.S.A. Journal of Petrology, 19, 317–340.

Rutter, E.H., and Brodie, K.H. (1988a) Experimental approaches to the study of deformation/metamorphism relationships. Mineralogical Magazine, 52, 35–42.

——— (1988b) Experimental "syntectonic" dehydration of serpentinite under conditions of controlled pore water pressure. Journal of Geophysical Research, 93, 4907–4932.

Spear, F.S., Ferry, J.M., and Rumble, D., III (1982) Analytical formulation of phase equilibria: The Gibbs method. Mineralogical Society of America Reviews in Mineralogy, 10, 105–152.

Spencer, K.J., and Lindsley, D.H. (1981) A solution model for coexisting iron-titanium oxides. American Mineralogist, 66, 1189–1201.

Turner, F.J. (1980) Metamorphic petrology: Mineralogical, field, and tectonic aspects, 2nd edition. McGraw-Hill, New York.

Verhoogen, J. (1951) The chemical potential of a stressed solid. American Geophysical Union Transactions, 32, 251–258.

Walder, J., and Nur, A. (1984) Porosity reduction and crustal pore pressure development. Journal of Geophysical Research, 89, 11,539–11,548.

Walther, J.V., and Orville, P.M. (1982) Rates of metamorphism and volatile production and transport in regional metamorphism. Contributions to Mineralogy and Petrology, 79, 252–257.

Watson, E.B., and Brenan, J.M. (1987) Fluids in the lithosphere. I: Experimentally determined wetting characteristics of CO_2-H_2O fluids and their implications for fluid transport, host-rock physical properties, and fluid-inclusion formation. Earth and Planetary Science Letters, 85, 497–515.

Wheeler, J. (1985) Thermodynamics of rocks under anisotropic stress: A discussion. Journal of the Geological Society, 142, 1242.

Winter, J.K., and Ghose, S. (1979) Thermal expansion and high-temperature crystal chemistry of the Al_2SiO_5 polymorphs. American Mineralogist, 64, 573–586.

Wood, B.J., and Walther, J.V. (1983) Rates of hydrothermal reactions. Science, 222, 413–415.

Manuscript received October 9, 1989
Manuscript accepted August 2, 1990